Thin Solid Films 520 (2012) 1842–1846

Contents lists available at SciVerse ScienceDirect

Thin Solid Films

journal homepage: www.elsevier.com/locate/tsf

In situ preparation of calcium carbonate films

S. Dahle [a,b], F. Voigts [b], W. Maus-Friedrichs [a,b,*]

[a] Clausthaler Zentrum für Materialtechnik, Technische Universität Clausthal, Leibnizstrasse 4, 38678 Clausthal-Zellerfeld, Germany
[b] Institut für Physik und Physikalische Technologien, Technische Universität Clausthal, Leibnizstrasse 4, 38678 Clausthal-Zellerfeld, Germany

ARTICLE INFO

Article history:
Received 6 April 2011
Received in revised form 26 August 2011
Accepted 30 August 2011
Available online 10 September 2011

Keywords:
Metastable Induced Electron Spectroscopy
Ultraviolet Photoelectron Spectroscopy
X-ray Photoelectron Spectroscopy
Calcium
Calcium oxide
Calcium carbonate
Carbon dioxide

ABSTRACT

The in situ preparation of calcium carbonate films in an ultra high vacuum (UHV) is inhibited by the decomposition of CO_2 molecules at the surface and the absence of CO_2 bulk diffusion. Therefore, it is not possible to prepare such films simply by CO_2 exposure to a calcium layer.
We investigated different approaches for the preparation of $CaCO_3$ films in an UHV. Among these, only the simultaneous evaporation of Ca atoms in a mixed O_2 and CO_2 atmosphere is able to produce well defined stoichiometric calcium carbonate films. Metastable Induced Electron Spectroscopy, Ultraviolet Photoelectron Spectroscopy and X-ray Photoelectron Spectroscopy are employed to verify quality and purity of the films.

1. Introduction

The thermal decomposition of calcium carbonate is of great technological importance mainly because of the manifold applications of burnt limestone. Nevertheless, no reaction model is able to describe the arbitrary limestone behavior of limestone during calcination completely up to now. The most promising approaches [1,2] take into account the mass transfer and diffusion via multiple paths as well as heat transfer, heat conduction, reaction rates, the heat of the reaction and the evolution of the product's pore structure. But even this is not perfectly adequate, for example the results of thermogravimetric analysis suggest an exponential dependence of the reaction rate as a function of the CO_2 partial pressure which does not fit the model [1]. Furthermore, the calcination process is affected by a varying number of intrinsic effects that are only partly known, for example the catalytic effect of alkali carbonates [3]. These intrinsic effects make it even more difficult to find a sufficient approach to describe the calcination process. Nevertheless, an all-embracing model would probably simplify industrial processing which may also lead to a significant conservation of energy. Further investigations of these reactions need to be carried out in a way that separates all these steps. One promising approach for such a separation is to start with pure films at thicknesses of several atomic layers under ultra high vacuum (UHV) conditions, thus excluding the formation of closed pores as well as the CO_2 back-diffusion. Extending these results by a stepwise increase of the film thickness, will cause additional effects to occur such as bulk diffusion, pore formation, diffusion in closed pores and others. In this way, improved models may be formulated that sufficiently describe the decomposition process.

The application of limestone as regenerative CO_2 sorbent has been discussed for several years, but all CaO based sorbents developed so far suffer from a decline in absorption capacity [4–6]. Even though some chemical and physical approaches to improve the stability were made [7], none of them was investigated fundamentally. Precipitated calcium carbonate (PCC) has been used as functional filler in polymer technology for many years [8]. The functionalization of the PCC particles in wet chemistry is mainly based on acids and aims at modifications restricted to the surface. For both applications, a study of the underlying processes by means of surface analytical methods may contribute to the understanding of the system and point out approaches for application improvements. The investigation on these substrates should separate all steps included in the carbonation such as the molecular reaction, bulk diffusion, pore diffusion, sintering and so on. As described for the calcination process, this can be carried out by starting with thin films under UHV conditions.

One particular interaction is of great interest in medical studies concerning osteoarthritis [9]. That is the formation of basic calcium phosphates as well as calcium pyrophosphate dehydrate and hydroxyapatite from solvated calcium carbonate and enzymes in aqueous solutions. Prevention methods against osteoarthritis may be found if the actual mechanisms of the generation of the given minerals were understood more precisely. Surface science is capable of identifying or excluding direct mechanisms such as ligand interchange or heterogeneous catalysis. An adequate model system for these studies would be a film of $CaCO_3$ when prepared thin enough to avoid charging. Though this investigation

* Corresponding author. Tel.: +49 5323 72 2310; fax: +49 5323 72 3600.
E-mail address: w.maus-friedrichs@pe.tu-clausthal.de (W. Maus-Friedrichs).

0040-6090/$ – see front matter
doi:10.1016/j.tsf.2011.08.112

of the occurring processes is envisaged, further preliminary studies concerning spectroscopical data on the enzymes involved are required.

The preparation of $CaCO_3$ films with thicknesses between a nanometer and a micrometer is required as basis for all of the future studies described above. Previous experiments on the adsorption of CO_2 and CO on Ca and CaO have shown that only one single surface layer of $CaCO_3$ is formed [10]. These first reaction products act as passivation layer sealing off the underlying bulk.

Therefore, the preparation of a $CaCO_3$ film via exposure of CO_2 to a Ca or CaO film is not working under vacuum conditions. Microscopic investigations suggest that the bulk carbonation reaction only takes place in the presence of water nano-droplets at room temperature [11]. Nevertheless, this is no suitable method to prepare $CaCO_3$ films for the given applications because of the influence of surface complexation [12] and structure modification from solution-precipitation-cycles [13] on the produced film.

In this paper we present a procedure for the fabrication of clean $CaCO_3$ films which can be used for fundamental future investigations of the calcination process. It is not within the scope of this paper to show any result of the investigations mentioned above, but to present a film preparation suitable to carry out these studies. We apply Metastable Induced Electron Spectroscopy (MIES), Ultraviolet Photoelectron Spectroscopy (UPS) and X-ray Photoelectron Spectroscopy (XPS) for the investigation of the $CaCO_3$ thin film formation.

2. Experimental details

An ultra high vacuum apparatus with a base pressure of 5×10^{-11} hPa is used to carry out the experiments [14]. All measurements were performed at room temperature.

Electron spectroscopy is performed using a hemispherical analyzer (VSW HA100) in combination with a source for metastable helium atoms (mainly $He^*\ ^3S_1$) and ultraviolet photons (HeI line). A commercial non-monochromatic X-ray source (Specs RQ20/38C) is utilized for XPS.

During XPS, X-ray photons irradiate the surface under an angle of 80° to the surface normal, illuminating a spot with a diameter of several mm. For all measurements presented here the Al K_α line (photon energy 1486.7 eV) is used. Electrons are recorded by the hemispherical analyzer with an energy resolution of 1.1 eV emitted under an angle of 10° to the surface normal. All XPS spectra are displayed as a function of binding energy with respect to the Fermi level.

For quantitative XPS analysis, photoelectron peak areas are calculated via mathematical fitting with Gauss-type profiles using OriginPro 7G including the PFM fitting module, which applies Levenberg–Marquardt algorithms to achieve the best agreement possible between experimental data and fit. Due to the plain background observed for the Ca 2p and O 1s structures, a linear background subtraction was applied before the fitting procedure. Peak widths (full width at half maximum, FWHM) and binding energies from preliminary experiments on CaO and $CaCO_3$ [10] were used as reference data for the fits, as well as additional literature [15,16]. Photoelectric cross sections as calculated by Scofield [17] and inelastic mean free paths from the NIST database [18] as well as the energy dependent transmission function of our hemispherical analyzer are taken into account when calculating stoichiometry. MIES and UPS are performed applying a cold cathode gas discharge via a two-stage pumping system. A time-of-flight technique is employed to separate electrons emitted by He* (MIES) from those caused by HeI (UPS) interaction with the surface. The combined He*/HeI beam strikes the sample surface under an angle of 45° to the surface normal and illuminates a spot with a diameter of approximately 2 mm. The spectra are recorded simultaneously by the hemispherical analyzer with an energy resolution of 220 meV under normal emission within 280 s acquisition time.

MIES is an extremely surface sensitive technique probing solely the outermost layer of the sample, because the He* atoms interact with the surface typically 0.3 to 0.5 nm in front of it. This may occur via a number of different mechanisms depending on surface electronic structure and work function, as described in detail elsewhere [19–21]. On the surfaces investigated here only Auger Deexcitation occurs. Here, an electron from the sample fills the 1s orbital of the impinging He*. Simultaneously, the He 2s electron carrying the excess energy is emitted. The resulting spectra reflect the surface density of states directly and can therefore be compared with UPS spectra directly.

MIES and UPS spectra are displayed as a function of the electron binding energy with respect to the Fermi level. The surface work function can be determined from the high binding energy onset of the MIES or the UPS spectra with an accuracy of ±0.1 eV.

Calcium (Sigma-Aldrich, 99%) was evaporated with a commercial UHV evaporator (Omicron EFM3).

The samples are exposed to O_2 (Linde Gas, 99.995%) and CO_2 (Linde Gas, 99.995%) via backfilling the chamber using a bakeable leak valve. The gas line is evacuated and can be heated in order to ensure cleanness. Additionally, a cold-trap is installed to minimize water contamination during gas dosage. A quadrupole mass spectrometer (Balzers QMS 112A) is used to monitor the partial pressure of the reactive gases simultaneously during all experiments.

3. Results

3.1. Film preparation and characterization

It is well known that the chemisorption of CO_2 on CaO surfaces leads to the formation of a complete carbonate monolayer on top of the surface with the underlying CaO remaining unaffected [10]. In this way it is not possible to produce thicker $CaCO_3$ layers.

The chemisorption of CO_2 on Ca leads to a total dissociation of the impinging molecules leading to the surface oxidation as primary step [10]. With increasing CO_2 exposure, the charge density below the Fermi level vanishes. Previous studies by Frigyes and Solymosi have shown that the dissociation of CO_2 most commonly proceeds via the formation of a CO_2^- anion. A vanishing charge density below the Fermi level diminishes the probability for a charge transfer from the surface to the molecule. That makes this dissociation path impossible, thus the probability for complete molecule dissociation decreases [10,22]. Again, further impinging CO_2 molecules form a carbonate monolayer. This procedure is also not suitable for the production of carbonate layers of more than one monolayer thickness. In addition, the total dissociation of the CO_2 molecules leads to adventitious carbon on the surface.

Therefore, the production of $CaCO_3$ films thicker than one layer requires a different approach. We evaporate calcium continuously in a mixed atmosphere of CO_2 and O_2, where the partial pressure of O_2 is more than two times as big as the partial pressure of CO_2. Therefore, the oxidation is mainly driven by the O_2 which has no influence on the subsequent carbonization by the CO_2. The partial pressures were adjusted according to the growth rate, leading to about 30 L O_2 per nm and about 70 L CO_2 per nm. These dosages are about 3 times as big as the saturation value determined for the chemisorption in preliminary experiments [10].

The simultaneous adsorption of O_2, CO_2 and Ca on Si(100) has been carried out by evaporating calcium at a flux of 100 nA in a mixed atmosphere of 3×10^{-7} hPa CO_2 and 7×10^{-7} hPa O_2 at room temperature. The water content of the residual gas never exceeded 7×10^{-9} hPa which is about 0.7% of the total pressure. The flux is a measure of the number of Ca ions (which are part of the Ca beam) moving towards the sample per second.

Fig. 1 shows XPS spectra of the C 1s and O 1s region of a film prepared as described above with an evaporation time of 10 min. The original data are plotted as black dots, the mathematical fit as described in Section 2 is displayed as the solid red line. The single Gaussians shown as dashed blue lines were gained by the fitting procedure as described in Section 2 without any constraints. The XPS measurements yield a final film thickness of 6.0 nm, evaluated by the attenuation of the Si 2p peak (not shown here), thus giving a growth rate of 0.6 nm/min. The C 1s structure consists of

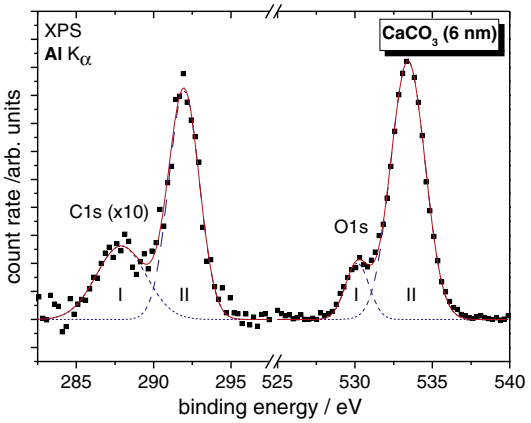

Fig. 1. XPS spectra of the C 1s and O 1s region of an in situ prepared $CaCO_3$ film with an evaporation time of 10 min (film thickness 6 nm). The binding energy axis features a break between 297.5 eV and 525.0 eV.

two Gaussians, the first with a binding energy of 287.9 eV denoted by I and a FWHM of 3.8 eV belonging to adventitious carbon [10,15]. It is believed to be due to different carbon–oxygen compounds [15]. Since the structure is quite broadened, more than one single carbon species seems to contribute. Thus, the exact chemical species can't be named. The second peak with a binding energy of 292.0 eV (peak II) and a FWHM of 2.3 eV can be assigned to carbonate groups [10,15,16,23–25]. The O 1s consists of an oxide species at 530.2 eV (peak I) with a FWHM of 1.8 eV and a carbonate species at 533.4 eV (peak II) with a FWHM of 2.6 eV [10]. All XPS C 1s data are summarized in Table 1 and all XPS O 1s data in Table 2 for better comparability.

Fig. 2 shows the MIES (a) and UPS (b) spectra of the same $CaCO_3$ film (solid black line) and a CaO film after adsorption of 81 L CO_2 (solid orange line) from preliminary experiments [10] for comparison. In the MIES spectra, a peak triplet at 14.4 eV, 11.9 eV and 7.1 eV is visible which has been assigned to carbonate groups before. The corresponding molecular orbitals (MOs) of the CO_3^{2-} groups are $1a'_2$, $1e'$, $4e'$ at 7.6 eV; $3e'$, $1a'_2$ at 12.1 eV and $4a'_1$ at 14.3 eV [23–25]. In UPS we find a similar carbonate triplet at 7.5 eV, 12.2 eV and 15.0 eV with an additional structure at 5.5 eV that can be identified as O 2p emission from calcium oxide. This peak points out that a small amount of oxide remains beneath the outermost layer of the film. It is much more significant for the CO_2 saturated CaO surface. Both MIES and UPS show a well defined band gap between the respective valence band maximum and the Fermi energy.

The oxide fraction of the $CaCO_3$ film is rather small for both UPS and XPS. All other structures fit quite well to the references for $CaCO_3$. Therefore, this film seems to be convenient for the further investigations illustrated in the introduction.

Fig. 3 shows XPS spectra of the C 1s and O 1s region of a $CaCO_3$ film prepared by evaporating calcium for 60 min at a flux of 100 nA in the mixed atmosphere of 3×10^{-7} hPa CO_2 and 7×10^{-7} hPa O_2. Again, the water content of the residual gas never exceeded 7×10^{-9} hPa which is about 0.7% of the total pressure. In contrast to the thin film described with Fig. 1, the underlying Si wafer is not visible in the XPS spectra any more. Therefore, the film thickness must be larger than the information depth of XPS. According to the growth rate determined for the thinner film (see Fig. 1) the thickness of this film should be about 36 nm. The spectrum of the C 1s region shows a first peak at 289.0 eV (I) with a FWHM of 4.2 eV and a second one at 292.9 eV (II) with a FWHM of 2.3 eV. Again, the second carbon species belongs to carbonate, the first one to adventitious carbon. The O 1s structure consists of an oxidic species at 531.1 eV (I) with a FWHM of 1.8 eV and a carbonate species at 534.4 eV (II) with a FWHM of 2.6 eV. The peak positions are shifted by about 1.0 eV towards higher binding energies because of a significant charging of the sample due to the isolating behavior of the thicker carbonate film.

The MIES and UPS spectra of this film suffer from the film charging and thus cannot be interpreted reasonably. Therefore, we do not show these spectra.

3.2. Natural limestone

Devonian lime material [26] from the Iberg in the middle of the Harz Mountains is used to check the films for their ability to serve as $CaCO_3$ model material. A fragment has been cut to a piece of about 1 cm^2 and polished down to a thickness of about 1 mm. The sample was rinsed with water to clean it from dust and afterwards transferred to the UHV chamber. No further cleaning has taken place in the apparatus.

Fig. 4a shows a XPS survey spectrum of the polished limestone sample. Besides the photoelectron peaks from calcium, carbon and oxygen, we find sodium, zinc and nitrogen as well as O(KLL) Auger emission.

Table 1
Summarized XPS results from the C 1s region.

System	Figure	Peak	Binding energy in eV	FWHM in eV	BE relative to Ca $2p_{3/2}$ in eV	Relative intensity	Assignment
CO_2/CaO/Si(100)	[13]	II	291.9	2.0	−55.9	1.00	Carbonate
$CaCO_3$/Si(100) (6 nm)	1	I	287.9	3.8	−60.6	0.34	–
		II	292.0	2.3	−56.5	0.66	Carbonate
$CaCO_3$/Si(100) (36 nm)	3	I	289.0	4.2	−60.6	0.31	–
		II	292.9	2.3	−56.7	0.69	Carbonate
Natural limestone	4	I	289.2	2.6	−62.3	0.74	–
		Ia	291.3	2.0	−60.2	0.08	–
		II	293.7	2.6	−57.8	0.18	Carbonate

Table 2
Summarized XPS results from the O 1s region.

System	Figure	Peak	Binding energy in eV	FWHM in eV	BE relative to Ca $2p_{3/2}$ in eV	Relative intensity	Assignment
CO_2/CaO/Si(100)	[13]	I	530.8	1.9	183.6	0.58	Oxide
		II	533.5	2.8	186.3	0.42	Carbonate
$CaCO_3$/Si(100) (6 nm)	1	I	530.2	2.2	181.7	0.15	Oxide
		II	533.4	2.6	184.9	0.85	Carbonate
$CaCO_3$/Si(100) (36 nm)	3	I	531.1	2.2	181.5	0.13	Oxide
		II	534.4	2.6	184.8	0.87	Carbonate
Natural limestone	4	II	535.9	2.7	184.4	0.94	Carbonate
		III	538.4	2.3	186.9	0.06	Hydrocarbons

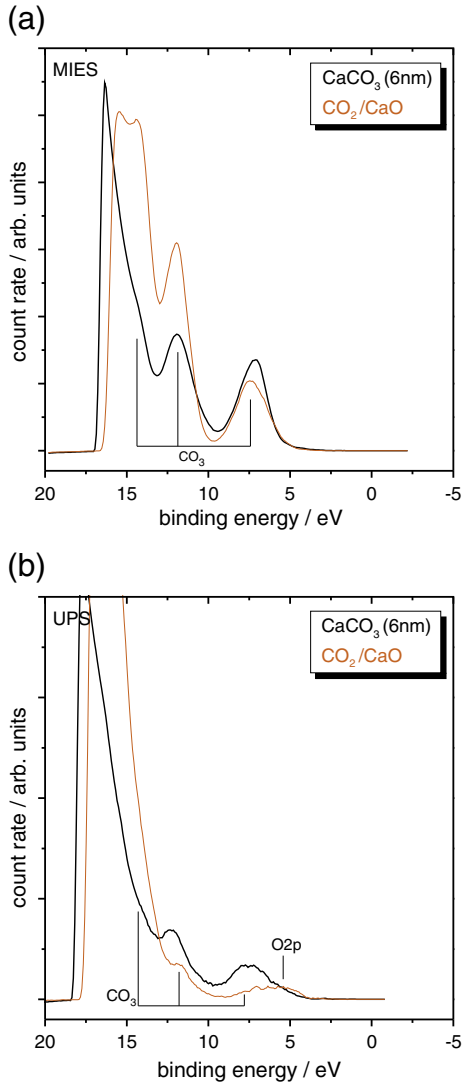

Fig. 2. MIES (a) and UPS (b) spectra of an in situ prepared $CaCO_3$ film with an evaporation time of 10 min (solid black line) and a CaO surface exposed to 81 L CO_2 (solid orange line, from [10]).

Calculating the global stoichiometry yields fractions of 7.5% for calcium, 32.6% for oxygen and 57.5% for carbon. Besides these main features, we find nitrogen to contribute with 2.0%, sodium with 0.2% and zinc with 0.2%. Any other impurity must be well below 1 at.%. Alkaline and earth alkaline metals are typical contaminations in limestones.

Fig. 4b shows XPS spectra of the C 1s and O 1s regions of the same sample. We find three species of carbon at 289.2 eV (I) with a FWHM of 2.6 eV, at 291.3 eV (Ia) with a FWHM of 2.0 eV and at 293.7 eV (II) with a FWHM of 2.6 eV. The first two species are due to contamination of adventitious carbon in the bulk that may originate in precipitation processes [15], the third one can be assigned to carbonate groups according to Section 3.1 and preliminary experiments [10]. In the O 1s region we only find two species. The first at a binding energy of 535.9 eV (II) with a FWHM of 2.7 eV can be assigned to oxygen in carbonate groups. The second one at 538.4 eV (III) with a FWHM of 2.3 eV may have originated in hydrocarbonate groups or carbonate complexes [15] that would likely form on limestone in humid environments [12,27]. Despite these surface contaminations, the results fit very well to the in situ prepared films. The charging effects on this sample prevent MIES and UPS measurements, as was the case for the thick film.

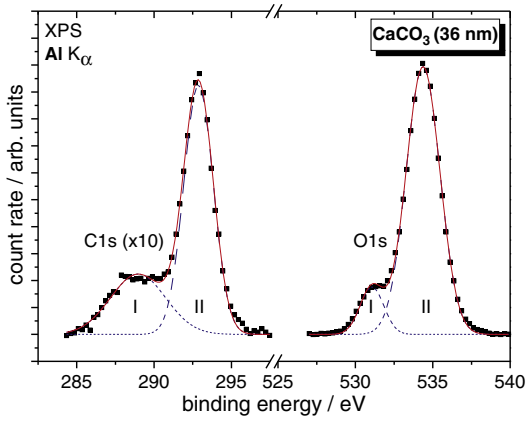

Fig. 3. XPS spectra of the C 1s and O 1s region of an in situ prepared $CaCO_3$ film with an evaporation time of 60 min (film thickness 36 nm). The binding energy axis features a break between 297.5 eV and 525.0 eV.

4. Discussion

The two $CaCO_3$ films with thicknesses of 6 nm (Figs. 1 and 2) and 36 nm (Fig. 3) prepared as described in the previous section show very similar structures in XPS, even though slightly shifted. The chemical shifts of the Ca 2p peaks during interaction of the Ca with O_2 or CO_2 are rather small [28] and are hardly measurable with XPS. Therefore, we use the Ca 2p peak as verification for the peak positions despite charging effects. The binding energies relative to the Ca $2p_{3/2}$ peak are 181.5 eV and 181.7 eV

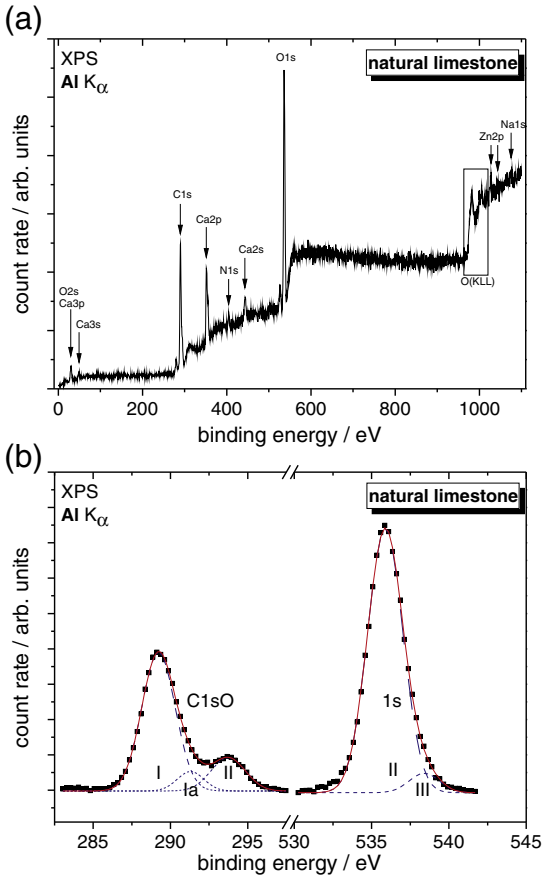

Fig. 4. XPS survey spectrum (a) and detail spectra of the C 1s and O 1s region (b) of a natural limestone. The detail spectra (b) scale up two regions from the survey spectrum (a), while recorded at better energy resolution. The binding energy axis in (b) features a break between 297.5 eV and 525.0 eV.

respectively for 6 nm and 36 nm for the O 1s oxide peaks (peaks II) and accordingly 184.8 eV and 184.9 eV respectively for 6 nm and 36 nm for the carbonate peaks (peaks II). The natural limestone yields a binding energy difference of 184.4 eV from Ca $2p_{3/2}$ to O 1s. This suggest that the XPS results from both films are comparable to results from natural limestone despite binding energy shifts due to charging.

The C 1s peaks belonging to the carbonate (peaks II) were found at 56.5 eV and 56.7 eV respectively below the Ca $2p_{3/2}$ peak for both films prepared. The chemisorption of CO_2 leads to a carbonate peak 55.9 eV below the Ca $2p_{3/2}$, whereas the natural limestone shows a binding energy difference of 57.8 eV.

All these data can be found in Tables 1 and 2. They fit quite well to the results for another two references. The investigation on industrial $CaCO_3$ powder in terms of PCC has been produced by pressing powder (Alfa Aesar, $CaCO_3$ 99.5%) with 300 bar thus obtaining a tablet sample. Ex-situ prepared powder samples show surface contaminations that reduce the significance of the results. Therefore, we do not show the spectra. The adsorption of CO_2 on CaO has been investigated earlier [10] and leads to the formation of surface carbonates that do not show charging effects. In XPS we find binding energy differences of 183.0 eV for the oxide peak and 185.0 eV for the carbonate peak of the O 1s structure relative to the Ca $2p_{3/2}$ peak. The C 1s carbonate peak is located 57.4 eV below the Ca $2p_{3/2}$ peak. These binding energy differences are given in Table 1. The binding energy distances are quite similar for the carbonate and oxide peaks in all systems, thus pointing out that the films produced in the manner as described in Section 3 resemble the $CaCO_3$ references quite well.

The oxide fractions of the films vary between 13% and 15% according to the XPS O 1s peak fitting results. Besides the CO_3^{2-} structures in the UPS spectra, we also find intensity at the O 2p binding energy position. This appears to be quite comparable to the XPS results though the quantification is not straightforward. The small oxide fraction may be reduced even more by lowering the evaporation rate of calcium. Nevertheless, this evaporation rate seems to be the only restraint to the thickness of the produced films. In addition, the regulation of the partial pressures during the growth of the film is hindered by the production of CO through the dissociation of CO_2 by active filaments in the mass spectrometer and the evaporator. These increasing CO fraction leads to carbon contamination from dissociation and should not exceed the magnitude of CO_2.

Even though a fraction of oxide seems to be unavoidable, the quality of the films should be sufficient for any following investigations of the calcination process illustrated in the introduction. Since no oxide fraction is visible in MIES, surface effects can be studied on pure carbonate surfaces. Bulk reactions will suffer from the oxide proportion within the bulk, but should be easily correctable concerning the calcination process.

As a next step to these results, the growth process is investigated. First microscopic results suggest a Stranski–Krastanov growth, but have to be evaluated further before being published.

5. Summary

We present a method to produce thin $CaCO_3$ films in an UHV by evaporating calcium in a combined atmosphere of O_2 and CO_2. MIES, UPS and XPS were applied to verify the quality of the films via comparison to previous results for the $CaCO_3$ surface layer formation on CaO films [10] as well as natural limestone. No intrinsic limitation for the film's thickness has been found besides the production time.

Acknowledgments

The authors gratefully acknowledge valuable technical assistance by Lienhard Wegewitz and Denise Yvonne Rehwagen.

References

[1] J. Khinast, Chem. Eng. Sci. 51 (1996) 623.
[2] B.R. Stanmore, P. Gilot, Fuel Process. Technol. 86 (2005) 1707.
[3] J.-M. Huang, Thermochim. Acta 115 (1987) 57.
[4] B. Feng, W. Liu, X. Li, H. An, Energy Fuels 20 (2006) 2417.
[5] G. Grasa, B. González, M. Alonso, J.C. Abanades, Energy Fuels 21 (2007) 3560.
[6] V. Manovic, E.J. Anthony, Energy Fuels 22 (2008) 1851.
[7] K.O. Albrecht, K.S. Wagenbach, J.A. Satrio, B.H. Shanks, T.D. Wheelock, Ind. Eng. Chem. Res. 47 (2008) 7841.
[8] G. Levita, A. Marchetti, A. Lazzeri, Polym. Compos. 10 (1989) 39.
[9] M. Fuerst, L. Lammers, Rheumatol. Int. 30 (2010) 623.
[10] F. Voigts, F. Bebensee, S. Dahle, K. Volgmann, W. Maus-Friedrichs, Surf. Sci. 603 (2009) 40.
[11] T. Yang, B. Keller, E. Magyari, K. Hametner, D. Günther, J. Mat. Sci. 38 (2003) 1909.
[12] P. van Capellen, L. Charlet, W. Stumm, P. Wersin, Geochim. Cosmochim. Acta 57 (1993) 3505.
[13] A. Wolter, S. Luger, G. Schaefer, ZKG International 57 (2004) 60.
[14] M. Frerichs, F. Voigts, W. Maus-Friedrichs, Appl. Surf. Sci. 253 (2006) 950.
[15] S.L. Stipp, M.F. Hochella, Geochim. Cosmochim. Acta 55 (1991) 1723.
[16] S. Campbell, P. Hollins, E. McCash, M.W. Roberts, J. Electron Spectrosc. Relat. Phenom. 39 (1986) 145.
[17] J.H. Scofield, J. Electron Spectrosc. Relat. Phenom. 8 (1976) 129.
[18] National Institute of Standards and Technology Electron Inelastic-Mean-Free-Path Database 1.1, http://www.nist.gov/srd/nist71.cfm.
[19] Y. Harada, S. Masuda, H. Ozaki, Chem. Rev. 97 (1997) 1897.
[20] H. Morgner, Adv. At., Mol., Opt. Phys. 42 (2000) 387.
[21] G. Ertl, J. Kuppers, Low Energy Electrons and Surface Chemistry, VCH Verlag, Weinheim, 1985.
[22] F. Solymosi, J. Mol. Catal. 65 (1991) 337.
[23] W. Maus-Friedrichs, A. Gunhold, M. Frerichs, V. Kempter, Surf. Sci. 488 (2001) 239.
[24] D. Ochs, B. Braun, W. Maus-Friedrichs, V. Kempter, Surf. Sci. 417 (1998) 406.
[25] Y. Fukuda, I. Toyoshima, Surf. Sci. 158 (1985) 482.
[26] W. Buggisch, S. Krumm, Facies 51 (2005) 566.
[27] J.S. Lardge, D.M. Duffy, M.J. Gillan, M. Watkins, J. Phys. Chem. C 114 (2010) 2664.
[28] P.A.W. van der Heide, J. Electron Spectrosc. Relat. Phenom. 151 (2006).